Reduction of EMI with Chaotic Space Vector Modulation in Direct Torque Control

Mehmet Emin Asker[1], Ahmet Bedri Ozer[2], Hasan Kurum[3]
[1]*Vocational Schools of Technical Sciences, Dicle University, 21280 Diyarbakir, Turkey*
[2]*Department of Computer Engineering, Firat University, 23119 Elazig, Turkey*
[3]*Department of Electrical and Electronics Engineering, Firat University, 23119 Elazig, Turkey*
measker@dicle.edu.tr

***Abstract*—In this paper a study is presented about the reduction of electromagnetic interference (EMI) in Direct Torque Control (DTC) method by the means of chaotic space vector modulation. Space Vector Modulated Direct Torque Control (SV-DTC) is a method developed to reduce current and moment fluctuations which stem from the hysteresis controllers used in classical DTC method. The switching frequency amplitude was changed chaotically in a Space Vector Modulated Direct Torque Control (FFSV-DTC) having a Fixed switching frequency, and Chaotic Space Vector Modulated Direct Torque Control (CAFSV-DTC) method having chaotic amplitude modulated switching frequency was obtained. CAFSV-DTC method was suggested to reduce EMI, acoustic noise and current harmonics which occur in FFSV-DTC method. For this purpose, the proposed CAFSV-DTC method, using a Permanent Magnet Synchronous Motor (PMSM) drive, is compared to Random Amplitude Frequency method (RSV-DTC) and FFSV-DTC. Simulation results indicate that the proposed method yields better results.**

***Index Terms*—Space vector pulse width modulation (SVM), electromagnetic interference (EMI), chaotic switching frequency, direct torque control (DTC).**

I. INTRODUCTION

PMSM has become really competitive to an asynchronous motor in terms of lifetime cost. This motor has recently become quite attractive due to its many advantages because magnets, instead of windings, are used for its rotor [1].

Phase inductance of surface mounted PMSM is less than induction motor. Thus, in PMSM, the effect of electromagnetic noise is greater when compared to the induction motor [2].

DTC method, a high-performance control method, was originally developed for asynchronous motor [3] and then it was applied to PMSM [4]. Fast torque response and its easy applicability are important advantages of this method because of the fact that all calculations are on a stationary coordinate system. In addition, it is less dependent on parameters because stator flux and torque are estimated by the means of current and voltage information and stator resistance. Variable and low switching frequency, acoustic noises, high torque and high flux ripples, sensitivity of stator resistance to temperature at low frequencies and integrator deviations can be considered as the disadvantages of conventional DTC method [5].

Many methods were used to improve the weaknesses of the conventional DTC method. Many studies have been conducted on SV-DTC developed by utilizing the advantages of SVM algorithm [6]–[8]. SV-DTC methods have features such as fixed switching frequency, low torque ripple and low current ripple. However, some other features are available such as excessive knowledge of parameters, rotary coordinate transformations and high computations [6]–[8].

All electrical systems have specific electromagnetic interference limits (*e.g.* CISPR 25). Inverters are one of the main sources of EMI in AC drive systems. Filters and shielding, classic EMI reduction methods bring extra size, weight and cost. The best option and resolution for EMI caused particularly by the transmission path is to prevent it from its source where it is generated [9].

There are many studies about the reduction of EMI on AC drive systems. Random PWM technique has been developed to suppress EMI in power converters [10]–[14]. It method would also be possible to reduce acoustic noise and mechanical vibration by the means of this method. Random PWM are carried out in various ways such as random switching frequency, random pulse position technique and random switching technique [10]. It was displayed that acoustic noise and EMI were suppressed by using random PWM technique in SVM algorithm [2]–[13], [15]–[16].

Methods having various switching frequencies like random or chaotic PWM are generally applied to induction motor. However, in this context, there are a limited number of researches about random PWM on a PMSM drive [2]–[13]. Studies using chaotic PWM in PMSM drives could not be found.

Chaotic PWM techniques are the ones developed as an alternative to the random PWM techniques.

Chaotic signal is obtained more easily than the random signal and it is also simpler to apply [17]. In literature, there exist various available techniques such as Chaotic sinusoidal PWM, Chaotic pulse position PWM, hybrid chaotic SPWM and chaotic SV-PWM methods [18]–[21].

Manuscript received 5 January, 2015; accepted 19 August, 2015.

Zheng *et al*., in their research, applied chaotic PWM methods to the induction motor drive, and indicated that EMI, acoustic noise and mechanical vibrations are reduced [19]–[20].

In this study, a chaotic CAFSV-DTC method with a switching frequency chaotically varying in a certain range has been developed for PMSM drive. It is showed that, in FFSV-DTC method, electromagnetic and acoustic noises stemming from fixed switching frequency are suppressed. This is done by the means of common mode (CM) and differential mode (DM) voltage power spectrums. In addition, harmonic analyses of the line current were applied to reinforce the effectiveness of the proposed method.

II. ELECTROMAGNETIC INTERFERENCE (EMI)

Current and voltage waveforms include harmonics at higher levels of energy above the main frequency in the radio frequency area power switches are opened and closed, because of the short-term rise and decline in current and voltage $\left(dV/dt, dI/dt\right)$. This effect is known as EMI.

EMI which spreads by scattering and transmission, is also harmful to human health as well as it negatively affects the performance of electrical and electronic devices. To reduce the effects of EMI solutions such as filters, shielding, and snubber circuit can be produced. However, it would be more beneficial and more effective to find solutions to the problem at its source.

EMI spreading via transmission path is comprised of two categories known as Common-mode (CM) and differential-mode (DM). CM currents are measured between phase and ground, and DM currents are those measured between the different phases of the inverter. These currents are strong sources of EMI [22].

The effects of CM and DM currents can be written in terms of voltage as it follows [13], [17]:

$$V_{CM} = \left(\frac{V_{A0} + V_{B0} + V_{C0}}{3}\right), \tag{1}$$

$$V_{DM} = V_{i0} - V_{j0}, (i, j = A, B, C). \tag{2}$$

There are several international standards such as IEC, VDE, CISSP and FCC to determine the upper limits for EMI. In addition, there are various institutions which determine and certify standards for EMI radiated by power electronic devices.

III. THE PROPOSED CHAOTIC SPACE VECTOR MODULATION

SVM method is based on the expression of inverter voltage on the stationary reference frame as space vector.

Space vector

$$\vec{V} = V\sim + jV = \frac{2(V_{A0}\overset{0}{a} + V_{B0}\overset{1}{a} + V_{C0}\overset{2}{a})}{3}, \tag{3}$$

where is ($a = e^{j\frac{2®}{3}}$).

There are eight possible cases of a three-phase inverter $\left(2^3\right)$. Two of them are zero vectors, and the other six are active state vectors; these six active vectors form a hexagon. Space vector modulation, for each switching cycle, creates a rotating reference vector approach by switching the two closest active-state and zero state vectors.

In order to achieve the best harmonic performance and minimum switching for each switch, switching sequence is set such that switching occurs on only one arm of the inverter, while passing from one state to the next.

Active state vectors can be expressed as follows

$$\vec{V}_k = \frac{2}{3} V_{dc} e^{j(k-1)\frac{®}{3}}, \tag{4}$$

where (k = 1,…6). The most important part of SVM is to calculate the active and zero state vectors durations for each switching period. These calculations are as follows [23]:

$$m = \frac{®}{2}\frac{V_{ref}}{V_{dc}}, \tag{5}$$

$$\begin{bmatrix} T_k \\ T_{k+1} \end{bmatrix} = m\frac{\sqrt{3}}{®} T_s \begin{bmatrix} \sin\left(\frac{k®}{3} - wt\right) \\ \sin\left(wt - \frac{(k-1)®}{3}\right) \end{bmatrix}, \tag{6}$$

$$T_0 = \frac{T_s}{2} - (T_k + T_{k+1}), \tag{7}$$

where V_{ref} , V_{dc} , m, T_k and T_{k+1}, T_0 and T_S shows space vector amplitude, DC voltage, modulation index, active state vector computation time, zero vector computation time and switching period respectively.

Chaotic switching frequency is obtained by changing the fixed switching frequency chaotically for chaotic SVM within a certain range. Chaotic change can be achieved by the help of a chaotic map or a chaotic oscillator. This study utilizes the logistic map. Logistic map, bifurcation diagram of which is presented in Fig. 1, displays chaotic behaviour at range of A $\left(3{,}57\text{-}4\right)$.

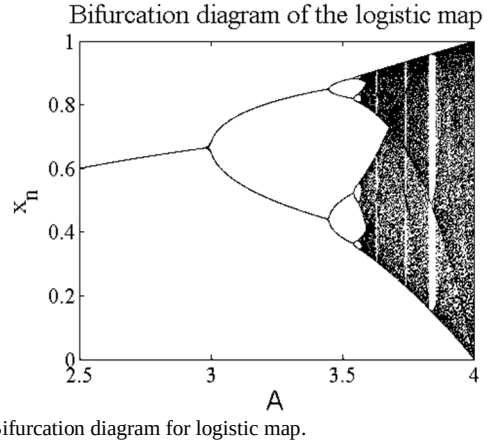

Fig. 1. Bifurcation diagram for logistic map.

Logistic map and chaotic amplitude frequency equations:

$$X_{n+1} = AX_n\left(1 - X_n\right), \tag{8}$$

$$f = f_{sw} + X_n \Delta f \sin\left(2® f_m t\right), \quad (9)$$

where f stands for real switching frequency, f_{sw} for fixed switching frequency, Δf for amount of frequency change, f_m for modulation frequency and X_n is for logistic map variable.

For calculating the chaotic switching frequency, chaotic amplitude modulation frequency is obtained by using the equation provided by (9) [19]–[20].

In algorithm for SVM modulation time calculation, as shown in (6), (7), the execution time of each vector varies depending on the switching period. Accordingly, when the SVM algorithm switching period is chaotic, SVM switching times for each sector will have reached a structure changing chaotically.

For chaotic SVM, the calculations related to the durations of chaotic switching periods for each sector are done according to (6), (7). Then, reference signals as shown in (10), (13) are obtained by means of these periods which change chaotically. Next, these changing chaotically reference signals are compared to a triangular wave which has period and height equal to that of chaotic switching period (T_S) and PWM signals for each sector are obtained. For single and double sectors is obtained PWM as shown in Fig. 2.

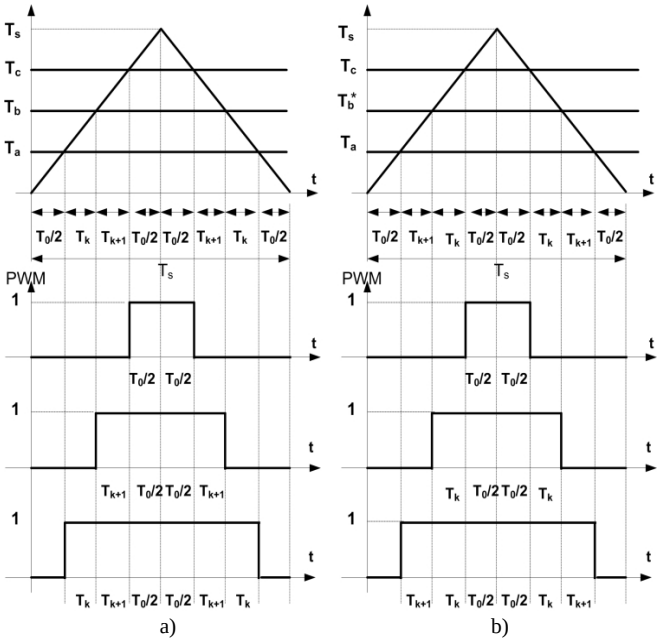

Fig. 2. Chaotic PWM signals for SVM in: a) Single numbered sectors; b) Double numbered sectors.

$$T_a = 2(T_o / 2), \quad (10)$$

$$T_b = 2(T_o / 2 + T_k), \quad (11)$$

$$T_b^* = 2(T_0 / 2 + T_{k+1}), \quad (12)$$

$$T_c = 2(T_o / 2 + T_k + T_{k+1}), \quad (13)$$

where T_k and T_{k+1} is active state vector computation time, T_0 is zero vector computation time respectively. T_a, T_b, T_b^* and T_c is amplitude of reference signals in single numbered sectors and double numbered sectors.

IV. CHAOTIC SV-DTC CONTROL METHOD

In conventional DTC method, the motor field and torque are estimated using the instantaneous values of the stator current and voltage. By the means of this information, in order to correct deviations from the torque and field references, control for each inverter is assumed by choosing the best switching cases out of a switching table. To choose from this table, sector information based on the position of stator field vector and field and torque controller output information are required. DTC structure is composed of two hysteresis controllers, field and torque estimator, voltage vector selector and the inverter.

Hysteresis bandwidths are highly effective on the motor behaviour in this method. The bandwidth, wide or narrow, influences the switching frequency and field waveform quality [4]. This is a method developed to improve the conventional DTC method, utilizing the SVM algorithm. It has the advantages of SVM method.

Classic DTC algorithm is based on motor field and torque and the digital control signals calculated for the inverter utilizing instantaneous values of the stator current and voltage. Algorithms used in SV- DTC control methods, however, is based on average values for the inverter switching signals of which are developed by SVM. This is the basic difference between the SV-DTC and DTC.

Different algorithms have been developed in SV-DTC method [5]. SV-DTC method having closed-loop torque control appropriate for PMSM is studied in this paper. In this method, block diagram provided in Fig. 3, current and voltage information and stator resistance information for field and torque estimation is required, as it is in conventional DTC method.

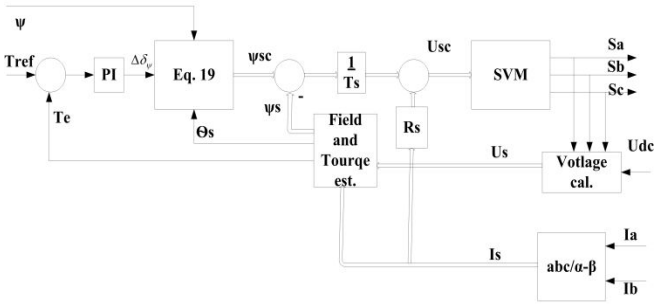

Fig. 3. The proposed block diagram of SV-DTC method [4].

Torque-based increase in angle, generated from the torque controller, and stator field position information are added as shown in (19), and α-β components of the reference stator field vector on the stator reference plane are obtained [5].

That is, an effective control process can be achieved because of the fact that increase in the load angle is directly reflected on the reference stator field.

The error obtained through comparing the reference stator flux and estimated stator flux is used to calculate stator voltage vector for space vectors. Calculations in SV-DTC method use (14)–(20).

Stator field components on the α-β axis, amplitude of the stator field space vector, angle and estimated torque can be calculated using the following equation:

$$\cdot_{\sim} = \int (V_{\sim} - RI_{\sim})dt, \quad (14)$$

$$\cdot \quad = \int (V \quad - RI \quad) dt, \tag{15}$$

$$\cdot_{\ s} = \sqrt{(\cdot_{\sim})^2 + (\cdot \quad)^2}, \tag{16}$$

$$^{-}_{S} = \tan^{-1}(\cdot \quad / \cdot_{\sim}), \tag{17}$$

$$T_e = \frac{2}{3} P(\cdot_{\sim} \times I \quad - \cdot \quad \times I_{\sim}), \tag{18}$$

$$\cdot_{sc} = \cdot (\cos(^{-}_{s} + \Delta\text{¢}. \ ) + \sin(^{-}_{s} + \Delta\text{¢}. \ ), \tag{19}$$

$$U_{SC} = \frac{1}{T_s} \Delta \cdot_{\ s} + I_s R_s, \tag{20}$$

where $V_{\sim}$ and V is for measured stator voltages, $I_{\sim}$ and I are for measured stator currents, $\cdot_{\sim}$ and $\cdot$ are for stator flux components, $\cdot_{\ S}$ is for stator flux amplitude, $^{-}_{S}$ is angle of the stator flux space vector, T_e is estimated torque, $\cdot_{SC}$ is calculated reference stator flux, $\Delta \cdot_{\ s}$ is stator flux error, $\cdot_{SC}$ is magnet flux, $\Delta\text{¢}.$ is torque induced load angle, U_{sc} is calculated space vector amplitude of stator voltage, I_s is measured stator current, R_s is stator resistance and T_s is system sampling period.

The method obtained by chaotically changing the amplitude of the frequency was named as CAFSV-DTC, the method having fixed switching was named as FFSV- DTC and the method frequency amplitude of which changes randomly was named as RSV-DTC. In this study a surface mounted PMSM is used. These motor parameters are presented in Table I.

V. SIMULATION RESULTS

Simulations were performed using Matlab Simulink. In this study, simulations are performed for FFSV-DTC, CAFSV-DTC and RSV- DTC. In Matlab program was used periodogram for power spectrum. On the simulations comparisons were made in terms of EMI, acoustic noise and current harmonics. For EMI value and acoustic noise, V_{CM} and V_{DM} 's power spectral density (PSD) values were analysed. Studies carried out in many countries for EMI values using PSD at 9 kHz–150 kHz range, which is a limitation determined by VDE. As for the acoustic noise, power spectrum peak values at the range of $(f - \Delta f)$ and $(f + \Delta f)$ indicates the acoustic noise levels [19]. In terms of current quality, line current harmonics were obtained and compared for three methods.

V_{CM} and V_{DM} power spectrums were obtained for each method as the motor was loaded by 5 N.m and using at reference speed of 63 rad/s. In addition, under same conditions, PSD values and the results of line current harmonics analysis are given.

The comparison is done in two stages.

1. EMI was compared according to the results obtained at 9 KHz–150 KHz range and maximum PSD values. High PSD values indicate high EMI. When the results, which were obtained as V_{CM} power spectrum, presented in Fig. 4, are analysed it is observed that it is 23 dB/Hz for FFSV-DTC, 2 dB/Hz for CAFSV-DTC and 4 dB/Hz for RSV-DTC. V_{DM} results, presented in Fig. 4, are as 20 dB/Hz for FFSV-DTC, 9 dB/Hz for CAFSV-DTC and 10 dB/Hz for RSV-DTC. It is an obvious finding that the proposed CAFSV- DTC method and RSV-DTC method provide very similar results; but both methods are much more effective when compared to FFSV-DTC method. Thus, it is shown that EMI value is decreased in the proposed CAFSV-DTC method having a chaotic switching frequency and RSV-DTC method having a random switching frequency.

In addition, to have an idea about acoustic noise in Fig. 4 values in the range of 4.5 KHz–7.5 KHz interval was checked over. When the values in this range were examined, it was determined that, CAFSV-DTC method is more effective than other methods.

2. It is a comparison made in terms of current quality. To do this, PSD values for the motor line current and the results for harmonic analysis are presented in Fig. 5 and Fig. 6. When these figures are analysed, for the switching frequency, it is observed that FFSV-DTC method provides higher harmonics than other methods. CAFSV-DTC and RSV-DTC methods seem to have close values, but CAFSV-DTC produces slightly better results.

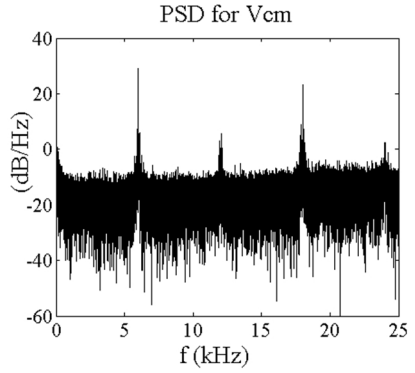

a)

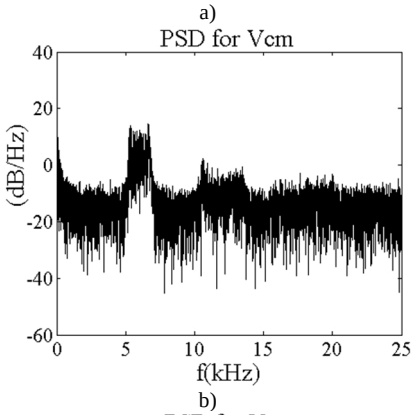

b)

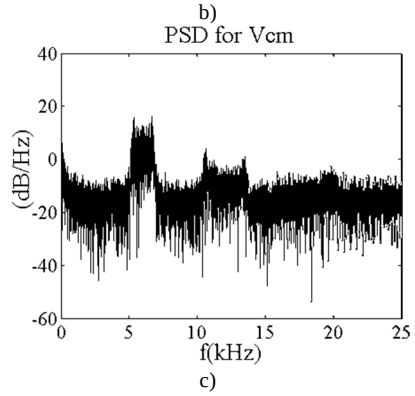

c)

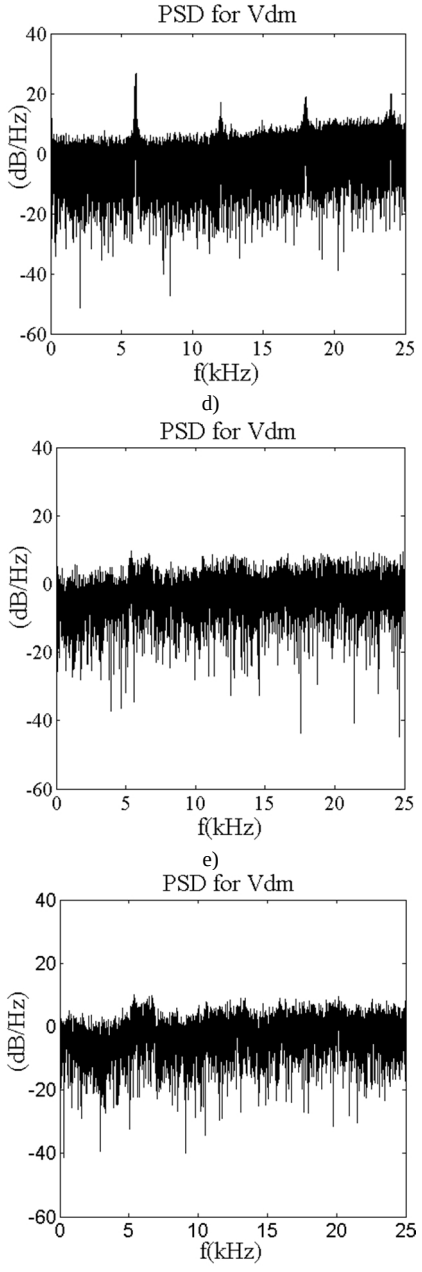

Fig. 4. Power Spectra for V_{CM} for: a) FFSV-DTC; b) CAFSV-DTC; c) RSV-DTC; Power Spectra for V_{DM} for: d) FFSV-DTC; e) CAFSV-DTC; f) RSV-DTC.

TABLE I. MOTOR PARAMETERS.

$\mathbf{R_s}$	0.41 Ω	**J**	0.0222 Kgm^2
$\mathbf{L_d}$	6.8 mH	**B**	0 Nms/rad
$\mathbf{L_q}$	6.8 mH	$\mathbf{U_N}$	220 V
P	2	$\mathbf{K_T}$	0.653 Nm/A

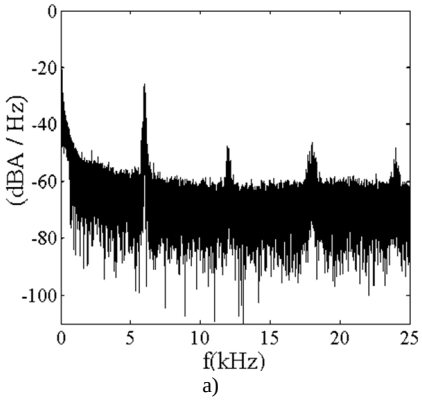

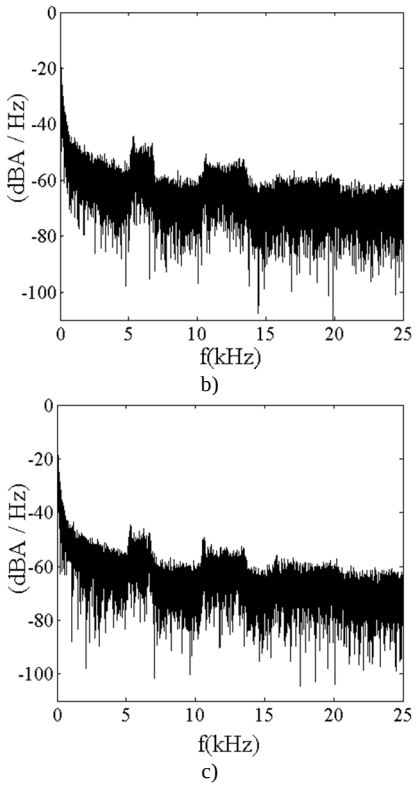

Fig. 5. Power Spectrum for Stator Current for: a) FFSV-DTC; b) CAFSV-DTC; c) RSV-DTC.

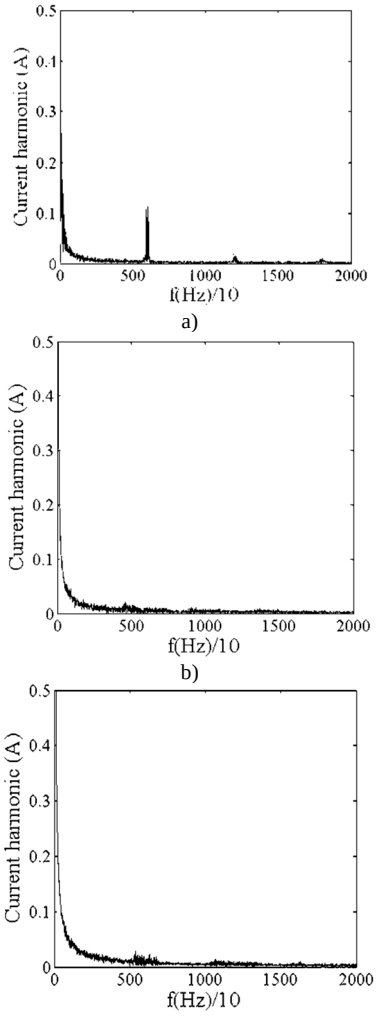

Fig. 6. Harmonic Analysis for Stator Current for: a) FFSV-DTC; b) CAFSV-DTC; c) RSV-DTC.

VI. CONCLUSIONS

In the simulations, SV-DTC methods switching frequency of which are fixed, chaotic and random are compared. In comparisons, EMI and acoustic noise levels in CAFSV-DTC and RSV- DTC are lower when compared to those of FFSV-DTC method. In addition, it is observed that the current harmonics around the switching frequency are also decreased in the proposed method. The results are close in chaotic modulation method and random modulation method. However, when compared to the chaotic signal, it is more difficult to obtain and apply random signal. Chaotic signal can be readily obtained from a chaotic oscillator, a chaotic map. Therefore it can be said that chaotic methods would be more efficient and convenient than other methods.

REFERENCES

[1] B. K. Bose, *Power Electronics And Motor Drives: Advances and Trends*. USA: Elsevier, 2006.

[2] Y. Xu, Q. Yuan, J. Zou, Y. Li, "Analysis of triangular periodic carrier frequency modulation on reducing electromagnetic noise of permanent magnet synchronous motor", *IEEE Trans. Magn*., vol. 48, no. 11, pp. 4424–4427, 2012. [Online]. Available: http://dx.doi.org/ 10.1109/TMAG.2012.2195643

[3] I. Takahashi, T. Noguchi, "A new quick-response and high-efficiency control strategy of an induction motor", *IEEE Trans. Ind. Appl.*, vol. IA-22, no. 5, pp. 820–827, 1986. [Online]. Available: http://dx.doi.org/10.1109/TIA.1986.4504799

[4] L. Zhong, M. Rahman, W. Hu, K. Lim, "Analysis of direct torque control in permanent magnet synchronous motor drives", *IEEE Trans. Power Electron*., vol. 12, no. 3, pp. 528–536, 1997. [Online]. Available: http://dx.doi.org/10.1109/63.575680

[5] G. S. Buja, M. P. Kazmierkowski, "Direct torque control of PWM inverter-fed AC motors-A survey", *IEEE Trans. Ind. Electron*., vol. 51, no. 4, pp. 744–757, 2004. [Online]. Available: http://dx.doi.org/10.1109/TIE.2004.831717

[6] C. Lascu, A. Trzynadlowski, "Combining the principles of sliding mode, direct torque control, and space-vector modulation in a highperformance sensorless ac drive", *IEEE Trans. Ind. Appl*., vol. 40, no. 1, pp. 170–177, 2004. [Online]. Available: http://dx.doi.org/10.1109/TIA.2003.821667

[7] L. Tang, L. Zhong, M. Rahman, Y. Hu, "A novel direct torque controlled interior permanent magnet synchronous machine drive with low ripple in flux and torque and fixed switching frequency", *IEEE Trans. Power Electron.*, vol. 19, no. 2, pp. 346–354, 2004. [Online]. Available: http://dx.doi.org/ 10.1109/TPEL.2003.823170

[8] G.-D. Andreescu, C. Pitic, F. Blaabjerg, I. Boldea, "Combined flux observer with signal injection enhancement for wide speed range sensorless direct torque control of IPMSM drives", *IEEE Trans. Energy Convers.*, vol. 23, no. 2, pp. 393–402, 2008. [Online]. Available: http://dx.doi.org/ 10.1109/TEC.2007.914386

[9] A. Fardoun Abbas, H. Ismail Esam, "Reduction of EMI in AC drives through dithering within limited switching frequency range", *IEEE Trans. Power Electron*., vol. 24, no. 3, pp. 804–811, 2009. [Online]. Available: http://dx.doi.org/ 10.1109/TPEL.2008.2002091

[10] R. L. Kirlin, S. Kwok, S. Legowski, A. M. Trzynadlowski, "Power spectra of a PWM inverter with randomized pulse position", *IEEE Trans. Power Electron*., vol. 9, no. 5, pp. 463–472, 1994. [Online]. Available: http://dx.doi.org/ 10.1109/63.321030

[11] K. S. Kim, Y. G. Jung, Y. C. Lim, "A new hybrid random PWM scheme", *IEEE Trans. Power Electron*., vol. 24, no. 1, pp. 192–200, 2009. [Online]. Available: http://dx.doi.org/10.1109/TPEL. 2008.2006613

[12] S. Kaboli, J. Mahdavi, A. Agah, "Application of random PWM technique for reducing the conducted electromagnetic emissions in active filters", *IEEE Trans. Ind. Electron*, vol. 54, no. 4, pp. 2333–2343,2007.[Online].Available:http://dx.doi.org/10.1109/TIE.2007.899944

[13] A. M. Hava, E Un, "Performance analysis of reduced common-mode voltage PWM methods and comparison with standard PWM methods for three-phase voltage-source inverters", *IEEE Trans. Power Electron*, vol. 24, no. 1, pp. 241–252, 2009. [Online]. Available: http://dx.doi.org/ 10.1109/TPEL.2008.2005719

[14] Y. C. Lim, S. O. Wi, J. N. Kim, Y. G. Jung, "A pseudorandom carrier modulation scheme", *IEEE Trans. Pow. Electron*, vol. 25, no. 4, pp. 797–805, 2010. [Online]. Available: http://dx.doi.org/

[15] J.-Y. Chai, Y.-H. Ho, Y.-C. Chang, C.-M. Liaw, "On acousticnoise reduction control using random switching technique for switchmode rectifiers in PMSM drive", *IEEE Trans. Ind. Electron*., vol. 55, no. 3, pp. 1295–1309, 2008. [Online]. Available: http://dx.doi.org/ 10.1109/TIE.2007.909759

[16] H. Khan, E. Miliani, K. E. K. Drissi, "Discontinuous random space vector modulation for electric drives: A digital approach", *IEEE Trans. Power Electron.*, vol. 27, no. 12, pp. 4944–4951, 2012. [Online]. Available: http://dx.doi.org/ 10.1109/TPEL.2012.2194511

[17] K. T. Chau, Z. Wang, *Chaos in Electric Drive Systems-Analysis, Control and Application*. Singapore: Wiley, 2011. [Online]. Available: http://dx.doi.org/10.1002/9780470826355

[18] H. Li, Y. Liu, J. Lu, T. Zheng, X. Yu, "Suppressing EMI in power converters via chaotic SPWM control based on spectrum analysis approach", *IEEE Trans. Ind. Electron.*, vol. 61, no. 11, pp. 6128–6136, 2014. [Online]. Available: http://dx.doi.org/10.1109/ TIE.2014.2308131

[19] Z. Wang, K. T. Chau, C. H. Liu, "Improvement of electromagnetic compatibility of motor drives using chaotic PWM", *IEEE Trans. Magn.*, vol. 43, pp. 2612–2614, 2007. [Online]. Available: http://dx.doi.org/ 10.1109/TMAG.2007.893712

[20] Z. Zhang, K. T. Chau, Z. Wang, W. Li, "Improvement of electromagnetic compatibility of motor drives using hybrid chaotic pulse width modulation", *IEEE Trans. Magn*., vol. 47, no. 10, pp. 4018–4021, 2011. [Online]. Available: http://dx.doi.org/ 10.1109/TMAG.2011.2152371

[21] H. Li, Z. Li, B. Zhang, F. Wang, N. Tan, W. A. Halang, "Design of analogue chaotic PWM for EMI suppression", *IEEE Trans. Electromagn.* vol. 52, no. 4, pp. 1001–1007, 2010. [Online]. Available: http://dx.doi.org/ 10.1109/TEMC.2010.2071878

[22] N. Mohan, *Power Electronics: Converters, Applications, and Design*. Wiley, 2003.

[23] Analog Devices, Implementing Space Vector Modulation With The ADMC401, 2000.